



ELSEVIER

## Status report of the PSI/ETH AMS facility

H.-A. Synal<sup>a,\*</sup>, G. Bonani<sup>b</sup>, M. Döbeli<sup>a</sup>, R.M. Ender<sup>b</sup>, P. Gartenmann<sup>b</sup>, P.W. Kubik<sup>a</sup>,  
Ch. Schnabel<sup>b</sup>, M. Suter<sup>b</sup>

<sup>a</sup> Paul Scherrer Institut, c/o ETH Hönggerberg, CH-8093 Zürich, Switzerland

<sup>b</sup> Institute of Particle Physics, ETH Hönggerberg, CH-8093 Zürich, Switzerland

### Abstract

The technical and operational details of the Zurich AMS system are discussed and an overview of new developments which have improved efficiency, sensitivity and accuracy of the measurements is given. The numerous applications associated with these measurements will not be covered.

### 1. Introduction

The PSI/ETH tandem accelerator laboratory has served as a multi-user multi-isotope AMS facility for more than 10 years. Since 1982 about 35 000 individual samples have been analysed for their <sup>10</sup>Be/Be, <sup>14</sup>C/C, <sup>26</sup>Al/Al, <sup>36</sup>Cl/Cl or <sup>129</sup>I/I isotopic ratios. During the past, the throughput has increased constantly and more than 4000 samples have been analysed per year in 1994 and 1995. In addition, a great variety of other long-lived radionuclides such as <sup>32</sup>Si, <sup>41</sup>Ca, <sup>59</sup>Ni, <sup>60</sup>Fe and <sup>126</sup>Sn have been analysed using AMS detection techniques. On the other hand, various ion beam techniques have been applied to analyse or to modify materials. At four different beam lines instruments have been set up for Rutherford Backscattering (RBS), channelling experiments, Nuclear Reaction Analysis (NRA), Particle Induced X-ray Emission (PIXE), Thin Layer Activation (TLA) and ion implantation. A floor plan of the facility is shown in Fig. 1. In the early years, the development of the Zurich AMS system has been covered in several progress reports [1–5]. More recently, new components have been added to the system and improvements have been made in connection with negative ion generation as well as with detection techniques of individual ions at high energies. These new developments are the motivation for this summary of the present status of the Zurich AMS facility.

### 2. The research facility

The system is based on an EN tandem accelerator. The accelerator is still working with its original belt charging

system and uses a CO<sub>2</sub>/N<sub>2</sub> mixture as insulation gas. Acceleration tubes have been replaced by Dowlish titanium electrodes, spirally inclined field tubes. With this configuration, routine operation is possible at terminal voltages up to 6 MV. The terminal voltage is controlled by a voltage stabilising system which uses the signals of a generating voltage meter, of a capacitive pick-up electrode and of a position sensitive Faraday cup, measuring the position of a pulsed ion beam in the focal plane of the AMS analysing magnet [3,6]. In the case of materials science experiments, when the ion beam is guided into the experimental hall, a slit stabilising system placed in the focal plane of the original HVEC 90° analysing magnet ( $R = 86.4$  cm, 70 MeV amu) is used to control the terminal voltage. The accelerator is equipped with a gas and a foil stripper [7,8]. The gas stripper incorporates a recirculating turbomolecular pump (280 l/s) and a Ti sublimation pump. Argon and nitrogen can be used as stripper gases; 3 μg/cm<sup>2</sup> carbon foils are used with the foil stripper. When nitrogen gas is used, the sublimation pump is turned on to improve the vacuum conditions in the acceleration tubes. For data transfer to and from the terminal an optical link is available. At present, three channels are used to read out the pressure in the stripper housing and the currents of the two terminal pumps [7].

A schematic diagram of the experimental arrangement at the low energy side of the accelerator is shown in Fig. 2. In the original setup, only one simple magnetic mass spectrometer had been used. The magnet ( $r = 30$  cm, 2.5 MeV amu) is equipped with a fast beam switching system [9,10,5] and permits the sequential injection of beams of various stable isotopes in pulses of 200 to 500 μs. This injector is used for routine AMS measurements of <sup>10</sup>Be and <sup>14</sup>C. A dedicated heavy ion spectrometer has been added for the injection of ion beams heavier than carbon [11]. This spectrometer combines a spherical 90° electro-

\* Corresponding author.

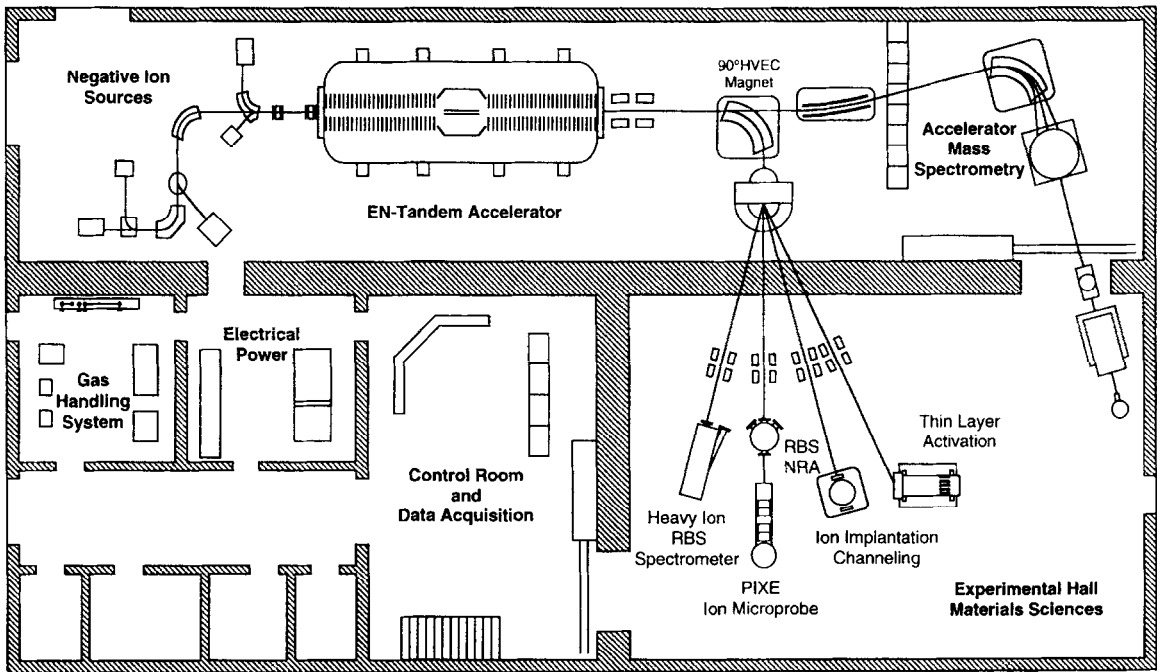


Fig. 1. Floor plan of the PSI/ETH accelerator facility. The system is based on an 6 MV EN tandem accelerator and is used for AMS (85%) and for materials sciences (15%).

static deflector ( $r = 75$  cm,  $E/\Delta E = 500$ ) and a stigmatic  $90^\circ$  dipole magnet ( $r = 56$  cm, 10 MeV amu). Pulsed beam operation is also possible with this injector. High voltage is applied to the vacuum chamber of the magnet via a

push-pull circuit of high voltage transistor switches. Hence, two pulses of arbitrary polarity with pulse lengths from  $20 \mu\text{s}$  to infinity are possible.

At both injection lines our standard caesium sputter

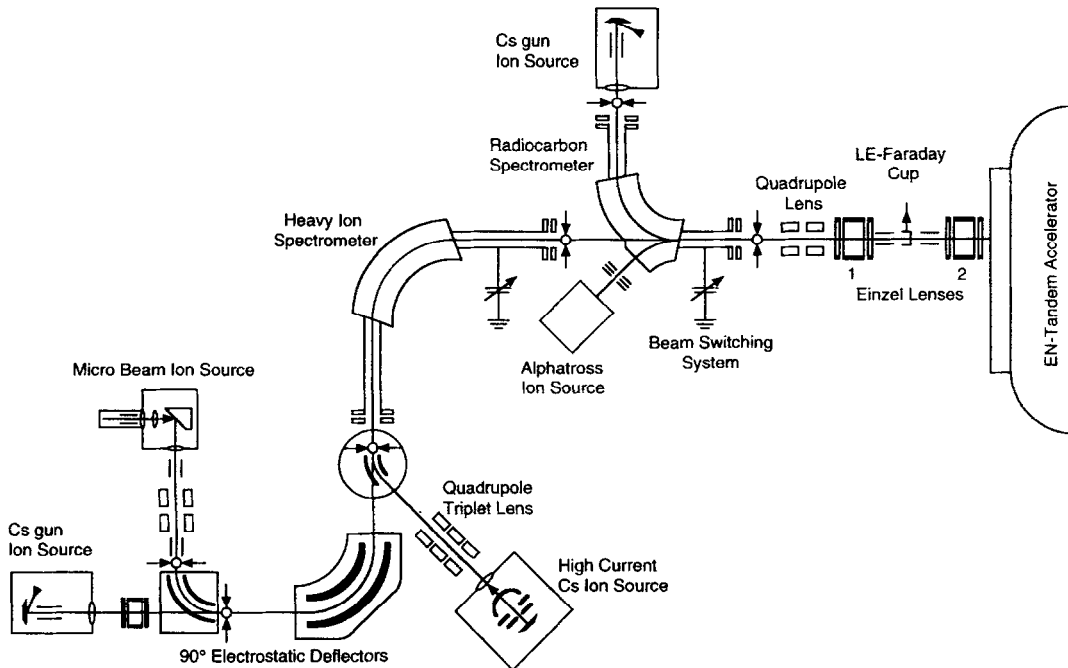


Fig. 2. Spectrometer set up at the low energy side of the EN tandem accelerator. Ion beams from five different negative ion sources can be injected into the accelerator.

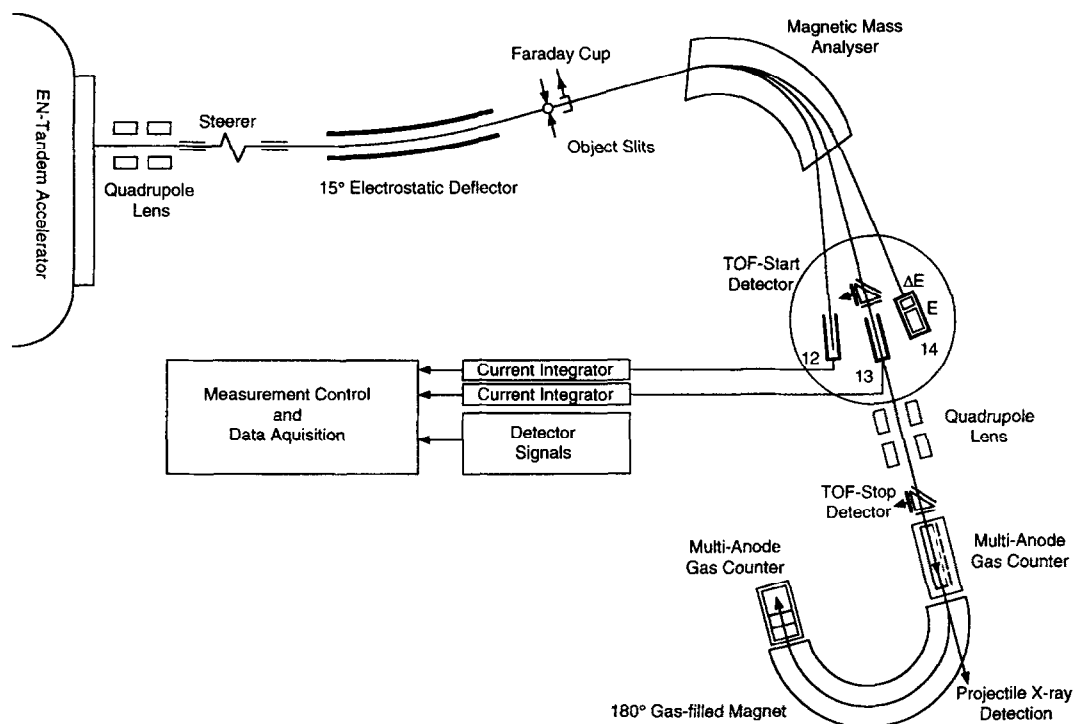


Fig. 3. High energy beam line of the AMS system. Only electrostatic beam guiding elements are used to perform mass independent beam transport to the high energy mass spectrometer. The 180° “gas-filled” magnet shown at the end of the AMS beam line deflects in the vertical plane.

source is installed utilising a caesium gun with a tungsten frit to produce the sputtering caesium beam [12]. The ion source box is at ground potential and can be accessed at any time during operation. A batch of 25 samples can be exchanged through a vacuum lock within 20 min without interrupting the measurement sequence. A wobbling mechanism is incorporated into the target holder assembly [5]. It allows a continuous movement of the sample holder across the sputtering caesium beam. It is used for  $^{14}\text{C}$  measurements to avoid fractionation caused by cratering effects during sputtering.

Also connected to the heavy ion injector now, is a high current Cs sputter source (HCS) using a spherical ioniser [13,14]. A cylindrical 40° electrostatic deflector is used in combination with an electrostatic quadrupole triplet lens to image the ion beam emerging from the HCS onto the injection line of the heavy ion injector. The deflector can be moved into position to select injection from the HCS or from the other sources connected to the heavy ion injector. The system has been used primarily for materials sciences experiments. In particular, ion implantation at high doses and of carbon cluster beams (i.e.  $\text{C}_2\text{--C}_8$  and  $\text{C}_{60}$ ) have been made [15]. In connection with AMS, the HCS has been used only for  $^{41}\text{Ca}$  measurements. At present, the stability and the reliability of the source are not sufficient to perform routine AMS measurements.

A new ion source with a micro-beam Cs gun (ATOMIKA<sup>1</sup>) has been added to the heavy ion injector [16]. This system can be used for stable trace element analysis exploiting AMS detection techniques. It had been shown in measurements with our standard ion source that detection limits of  $10^{-9}$  can be achieved for many elements, with the sensitivity being limited in many cases by contamination in the ion source [17]. Therefore, the new ion source is set up in an ultra high vacuum environment. More details can be found in Ref. [18]. The ion source is connected to the heavy ion injection line via an electrostatic 90° spherical deflector. This device can be retracted out of the beam path to enable injection from the standard ion source of the heavy ion injector. Thus, a pilot beam can be used to optimise the settings of the magnets and to calibrate the gas ionisation detector. In addition, a RF-ion source (NEC alphas<sup>2</sup>) is connected to the 45° port of the original injection magnet. This source is used for alpha and proton beams in connection with applications in materials sciences.

<sup>1</sup> Atomika Instruments, Bruckmannring 40, D-85764 Ober-schleißheim, Germany.

<sup>2</sup> National Electrostatics Corp., GraberRoad, Box 310, Middleton, Wisconsin 53562, USA.

Table 1

Details on the different radionuclide ion beams analysed at the Zürich AMS facility. The applied isobar separation technique is given in the last column: GIC: Gas Ionisation Chamber, NIF: Negative Ion Formation, GFM: "Gas-Filled" Magnet and PXD: Particle X-ray Detection

Radio-nuclide	Extracted ion	Typical negative ion current [ $\mu\text{A}$ ]	Terminal voltage [MV]	Charge state	Stripper	Typical transmission [%]	Ion energy [MeV]	Background	Isobar separation technique
$^{10}\text{Be}$	$\text{BeO}^-$	0.5–1.0	5.3	3+	Ar-gas	20	18	$< 10^{-14}$	Absorber/GIC
$^{14}\text{C}$	$\text{C}^-$	15–25	5.2	4+	Ar-gas	40	26	$< 10^{-15}$	NIF/GIC
$^{26}\text{Al}$	$\text{Al}^-$	0.1–0.2	5.7	5+	Ar-gas	10	34.2	$5 \times 10^{-14}$	NIF/GIC
$^{32}\text{Si}$	$\text{Si}^-$	5–10	6	7+	C-foil	10	48	$< 10^{-15}$	GFM/GIC
$^{36}\text{Cl}$	$\text{Cl}^-$	10–15	6	7+	C-foil	10	48	$< 10^{-15}$	GIC
$^{41}\text{Ca}$	$\text{CaH}_3^-$	0.3–0.5	6	7+	C-foil	5	47.6	$10^{-13}$	NIF/GIC
$^{59}\text{Ni}$	$\text{Ni}^-$	0.15–0.3	6	11+	C-foil	1	72	$< 10^{-9}$	GIC
$^{60}\text{Fe}$	$\text{FeH}^-$	0.02–0.03	6	9+	C-foil	5	59.9	$10^{-11}$	NIF/GIC
$^{126}\text{Sn}$	$\text{Sn}^-$	0.02–0.05	5	5+	Ar-gas	3	30	$10^{-7}$	PXD
$^{129}\text{I}$	$\text{I}^-$	5–10	4.7	5+	Ar-gas	3	28.2	$5 \times 10^{-14}$	NIF/GIC

An overview of the experimental set-up at the high energy side is shown in Fig. 3. At the high energy side only electrostatic beam optic elements are used to perform a mass independent beam transport. A  $15^\circ$  electrostatic deflector ( $r = 5.8$  m,  $E/q = 10$  MV) is used in combination with a quadrupole lens to focus the ion beam of the selected charge state onto the object slits of the following mass spectrometer. Mass separation is performed with a stigmatic  $90^\circ$  dipole magnet ( $r = 1.1$  m, 165 MeV amu). A large detection chamber having a mass acceptance of  $M/\Delta M = 6.5$  is placed in the focal plane of this magnet.

Several techniques can be applied to detect the analysed beams, to identify radionuclides and to separate isobars. The pulsed ion beams from the sequentially injected stable isotopes are stopped in Faraday cups and are measured with current integrators. Depending on the pulse length, beam currents down to a few pA can be measured. The standard technique for single ion detection uses a gas ionisation chamber to measure the specific energy loss of the ions stopped. In case of  $^{14}\text{C}$  measurements, this detector is placed inside the detection chamber. For the detection of  $^{26}\text{Al}$ ,  $^{36}\text{Cl}$ ,  $^{40}\text{Ca}$  and  $^{129}\text{I}$  a multi-anode gas ionisation detector is used [19]. It is connected to the beam line approximately 4 m behind the detection chamber on the  $90^\circ$  axis of the high energy magnet. The ion beam is focused onto the detector entrance by a magnetic quadrupole lens. A  $180^\circ$  "gas-filled" magnet ( $r = 60$  cm, 25 MeV amu) is available as an additional isobar separator [20] or, if it is operated without gas as a  $p/q$  filter. It is used for  $^{10}\text{Be}$ ,  $^{32}\text{Si}$ ,  $^{59}\text{Ni}$  and  $^{60}\text{Fe}$  detection in combination with a multi-anode gas ionisation detector. At the  $0^\circ$  port of the "gas-filled" magnet a system for the projectile X-ray detection (PXD) is set up. A Si(Li) detector is connected directly to the beam line vacuum system [21]. In addition, a time-of-flight system ( $l = 4$  m) [19] can be put into operation to improve stable isotope suppression. Secondary electron emission detectors are used to generate the

start and stop pulses. The start detector is positioned in the detection chamber, the stop detector is positioned directly in front of the first multi-anode detector. An intrinsic time resolution of 300 ps (FWHM) at about 80% total detection efficiency has been achieved with this system.

### 2.1. Accelerator control and data acquisition

All power supplies of the system can be set and monitored via a control panel [22]. The control system has been renovated and is now controlled by personal computer. The machine settings for the different isotope beams are stored in a data base and can be used as initial values for the beam tuning. In addition, calibration data for the most important beam optical elements, such as magnets, electrostatic deflectors and lenses exist and can be accessed by the control programme. Thus, the beam parameters for several elements can be set directly for a desired ion beam.

A new data acquisition system has been developed for routine AMS measurements. It is based on a UNIX work station and uses a VME front-end system for the acquisition of the experimental data. The incoming data are digitised in VME-ADCs (CAEN-V419) and scalers (CAEN-V260), processed and stored as spectra inside the memory of the VME front-end CPU module. The connection to the UNIX system is made via an ethernet link and data exchange is controlled by remote procedure calls. On the UNIX system all relevant measurement data are stored in an ORACLE database. Measured spectra are analysed using PV-Wave graphics library tools and are stored on disk for each measurement cycle. A graphical user interface is used for the communication to the measurement programme which controls automatically the measurement sequence. It provides, on line, all necessary information on results and status of the measurement to the operator and monitors important measuring parameters, such as transmission, beam currents and stable isotope ratios.

### 3. Routine measurement operation

The radionuclides  $^{10}\text{Be}$ ,  $^{14}\text{C}$ ,  $^{26}\text{Al}$ ,  $^{36}\text{Cl}$  and  $^{129}\text{I}$  are analysed routinely. Details on the operating conditions of the different radionuclides are given in Table 1.

#### 3.1. $^{10}\text{Be}$ measurements

For the detection of  $^{10}\text{Be}$ ,  $\text{BeO}^-$  molecules are injected into the accelerator. 5.3 MV terminal voltage and charge state 3+ (Ar gas stripper) are selected.  $^{10}\text{B}$  ions are the principal interference in the detection of  $^{10}\text{Be}$ . Due to its higher stopping power,  $^{10}\text{B}$  can be stopped completely in a passive absorber cell placed directly in front of the  $^{10}\text{Be}$  detector.  $^7\text{Be}$  background can be produced by the nuclear reaction  $^1\text{H} (^{10}\text{B}, \alpha) ^7\text{Be}$  taking place in the entrance foil of the gas ionisation chamber. To reduce this background, the mass 10 ion beam is sent to the “gas-filled” magnet which is used in this particular case as a  $p/q$  filter. At its entrance a 10–20  $\mu\text{g}/\text{cm}^2$  carbon foil is placed to post-strip the  $^{10}\text{Be}$  and the  $^{10}\text{B}$  ions. At energies of 18 MeV  $^{10}\text{Be}$  is stripped mainly into charge state 4+, whereas the highest stripping yield for  $^{10}\text{B}$  ions is the 5+ charge state. The background from  $^{10}\text{B}$  can thus be reduced at least by a factor of 5. An improved detector configuration allows better separation of  $^{10}\text{Be}$  and the interfering  $^7\text{Be}$ . A background correlation function is established using reduced counting rates from a pure boron oxide sample. It has been found that the actual  $^7\text{Be}$  counts, produced by  $^{10}\text{B}$  in the absorber entrance foil give a more reliable correlation to observed background events than the  $^{10}\text{B}$  current from the absorber cell ionisation chamber. The  $^7\text{Be}$  is measured for each sample in parallel with the  $^{10}\text{Be}$  in the same detector. Thus, there is now rarely a background exceeding 5% for sample ratios exceeding  $10^{-13}$ . For normalisation  $^9\text{Be}^{16}\text{O}$  molecules are injected in 260  $\mu\text{s}$  pulses (12.5 Hz) and the  $^{16}\text{O}^{5+}$  beam is measured with a Faraday cup inside the detection chamber after the high energy magnet. The actual current integration time is 200  $\mu\text{s}$ . The current integration is started as soon as the beam pulse has reached a constant value. The large spatial separation of  $^9\text{Be}$  and  $^{10}\text{Be}$  ion beams in the focal plane of the high energy magnet prevents the measurement of the  $^9\text{Be}^{3+}$  beam when the  $^{10}\text{Be}$  beam is adjusted to the  $90^\circ$  axis of the magnet. The almost exact  $E/q$  ratios of  $^{10}\text{Be}^{3+}$  and  $^{16}\text{O}^{5+}$  beams enables a simultaneous beam transport.

#### 3.2. $^{14}\text{C}$ measurements

Radiocarbon measurements are performed at 26 MeV (5.2 MV, 4+ charge state, Ar gas stripper). The two stable carbon isotopes  $^{12}\text{C}$  and  $^{13}\text{C}$  are injected with a pulse repetition rate of 12.5 Hz into the accelerator in 180 and 300  $\mu\text{s}$  pulses, respectively. Beam currents are integrated at the time of the beam pulse when a stable beam current has been reached for 20  $\mu\text{s}$  in the case of  $^{12}\text{C}$  and for 200  $\mu\text{s}$  in the case of  $^{13}\text{C}$ . In order to reduce loading

effects on the accelerator, pulsing of the steerer inside the ion source box has been introduced [5]. The ion beam is switched off before the voltage is applied to vacuum chamber of the magnet and is switched on as soon as the final voltage is reached (switching time 2  $\mu\text{s}$ ). Thus, the stable isotope ratio  $^{13}\text{C}/^{12}\text{C}$  is measured in the same sequence as the  $^{14}\text{C}/^{12}\text{C}$  ratio. Since the measurement of the currents from the stable isotopes are not affected by counting statistics, the measurement of the  $^{13}\text{C}/^{12}\text{C}$  ratio gives a good measure of the systematic uncertainties. Measurements of samples which have been analysed for their  $^{13}\text{C}/^{12}\text{C}$  ratios with conventional mass spectrometry have shown that the AMS results agree with the conventional ratios at the 1‰ uncertainty level [23,24]. For all analysed samples the AMS measured  $^{13}\text{C}/^{12}\text{C}$  ratio is used for the  $\delta^{13}\text{C}$  correction of the natural fractionation.

#### 3.3. $^{26}\text{Al}$ , $^{36}\text{Cl}$ and $^{129}\text{I}$ measurements

For radionuclides heavier than radiocarbon the heavy ion injection line is used. In case of  $^{26}\text{Al}$ , a  $\text{Al}^-$  ion current of typically 50–150 nA is extracted from our standard ion source. The terminal voltage is set to 5.7 MV and gas stripping is used to achieve charge state 5+ with about 30% stripping yield. The overall transmission is about 10%. 300  $\mu\text{s}$   $^{27}\text{Al}$  beam pulses are injected at a repetition rate of 25 Hz and are measured with a Faraday cup for a period of 200  $\mu\text{s}$  for normalisation. The  $^{26}\text{Al}$  ions are detected with the multi-anode ionisation chamber.

The isobar  $^{36}\text{S}$  interferes with the detection of  $^{36}\text{Cl}$ . In order to achieve high isobar separation, measurements are performed at the maximum terminal voltage of our EN Tandem. At 6 MV, 48 MeV is reached by selecting the charge state 7+ . 3  $\mu\text{g}/\text{cm}^2$  carbon foils are used yielding about 33% stripping efficiency. The resulting overall transmission is about 10%.  $^{35}\text{Cl}$  and  $^{37}\text{Cl}$  beam pulses (each 20  $\mu\text{s}$ ; 12.5 Hz) are injected and measured at the high energy side. The  $^{35}\text{Cl}$  beam is used for normalisation; the  $^{37}\text{Cl}/^{35}\text{Cl}$  ratio is analysed to control isotope fractionation effects. Four  $\Delta E$  signals and one  $E_{\text{tot}}$  signal are analysed to perform  $^{36}\text{Cl}/^{36}\text{S}$  isobar separation. The resulting background level is less than  $10^{-15}$ . More details can be found in Ref. [25].

$^{129}\text{I}$  measurements are made at 4.7 MV terminal voltage. By using gas stripping and selecting charge state 5+ a transmission of 3% is typical.  $^{129}\text{I}$  detection does not have isobaric ion interferences, but  $^{128}\text{Te}$  ions, which are injected as  $\text{TeH}^-$  together with the  $^{129}\text{I}$  ions, can cause unwanted background, because the Te/I separation is virtually impossible at 30 MeV with ionisation detectors. In order to increase the mass selectivity, a time-of-flight spectrometer is used. For additional information see [26]. Measurements of Woodward iodine<sup>3</sup>, the best commer-

<sup>3</sup> Woodward Iodine Corporation, Woodward, Oklahoma, USA.

cially available  $^{129}\text{I}$  blank material, have resulted in a  $^{129}\text{I}/\text{I}$  ratio of  $5 \times 10^{-14}$ , with mass 128 being clearly separated from a residual mass 129 peak in the observed time-of-flight spectra. At present, a new  $^{129}\text{I}$  time-of-flight spectrometer is under construction. Since time resolution is sufficient, this system will have a shorter flight path and an ionisation detector with a larger acceptance can be used.

#### 4. Measurements of other heavy radionuclides

$^{32}\text{Si}$  measurements have been made using the “gas-filled” magnetic spectrometer to suppress interference by  $^{32}\text{S}$ . In order to achieve a high beam energy, the accelerator is operated at 6 MV terminal voltage and charge state 7+ is selected to obtain a high stripping yield. Using the “gas-filled” magnet in combination with a multi-anode gas ionisation chamber a  $^{32}\text{S}$  suppression of 11 orders of magnitudes has been reached. To test the  $^{32}\text{S}$  suppression of the detection system a 0.3 nA  $^{32}\text{S}^{7+}$  ion beam has been injected into the “gas-filled” magnet for 15 min. Only two  $^{32}\text{S}$  events have been misidentified in the gates where  $^{32}\text{Si}$  are to be expected. This corresponds to a  $^{32}\text{Si}/\text{Si}$  background ratio of less than  $10^{-15}$ . A standard dilution series with  $^{32}\text{Si}/\text{Si}$  ratios between  $2 \times 10^{-13}$  and  $1.75 \times 10^{-10}$  have reproduced in AMS measurements at the 5% uncertainty level.

For the detection of  $^{41}\text{Ca}$ , the accelerator is operated at 6 MV terminal voltage, and charge state 7+ (foil stripping) is used.  $\text{CaH}_3^-$  ions are extracted from the ion source (HCS: 300–500 nA) in order to eliminate isobaric interferences from potassium which does not form  $\text{KH}_3^-$  ions. Particle identification is made with the multi-anode ionisation chamber. The time-of-flight spectrometer is used to improve mass separation. In particular,  $^{42}\text{Ca}$  and  $^{43}\text{Ca}$  ions which are injected as hydrides at mass 44 can be suppressed efficiently. At present a detection limit of  $10^{-13}$  has been achieved. More information can be found in Ref. [27].

Beside routine operation of our AMS system, a significant fraction of beam time is used for new developments. In particular, new techniques for isobar separation have been researched. The detection of characteristic projectile X-rays (PXD) has been proposed as a new isobar separation technique [28]. In case of Cl/S, Ni/Co and Sn/Te, the potential of PXD has been elaborated with respect to its isobaric separation power [22,29]. In contrast to single ion detection with gas ionisation chambers or semiconductor detectors, the detection of projectile X-ray has a detection efficiency smaller than 1. An appropriate selection of projectile and target combination can result in an increase of X-ray yield due to orbital matching effects [30]. However, at projectile energies below 50 MeV, the total X-ray yield of Ni and Sn ions will not exceed 15%. On the other

hand, isobar separation is independent of the beam energy and even with small accelerators a suppression of heavy isobars is possible.

In the case of  $^{59}\text{Ni}/^{59}\text{Co}$  separation at 18 MeV beam energy, a detection limit of  $^{59}\text{Ni}/\text{Ni} = 10^{-8}$  has been achieved [29]. However, this is substantially higher than the background level obtained at 72 MeV, the maximum energy which can be reached by the EN tandem accelerator for Ni ions ( $U_T = 6$  MV; charge state 11+) using a multi-anode gas ionisation chamber for isobar suppression [29].

Another field of activity is the measurement of absolute radionuclide concentrations in connection with half-life determinations. First experiments were made with  $^{32}\text{Si}$  [31]. More recently, a new attempt was made to measure the half-life of  $^{126}\text{Sn}$  [32,33]. The primary difficulty in the determination of the  $^{126}\text{Sn}$  concentration is the interfering stable isobar  $^{126}\text{Te}$ . At energies available at the EN tandem accelerator, no reasonable isobar separation with a gas ionisation detector can be expected. Hence, the PXD technique was used to measure the  $^{126}\text{Sn}/^{126}\text{Te}$  ratio of the samples. In addition, two pulsed beams of different stable Sn isotopes were used to measure the absolute detection efficiency of the PXD set-up. Independently, the  $^{126}\text{Sn}/\text{Sn}$  ratio was measured using a gas ionisation chamber for the detection of ions of mass 126. To account for the  $^{126}\text{Te}$  background, the previously measured  $^{126}\text{Sn}/^{126}\text{Te}$  ratio was applied as background correction. Within the experimental uncertainties the same  $^{126}\text{Sn}/\text{Sn}$  ratio was obtained with both methods [33].

Test measurements have been made to evaluate detection limits of  $^{60}\text{Fe}/\text{Fe}$  ratio at low beam energies. With foil stripping, charge state 9+ gives a reasonable stripping yield for iron at 6 MV terminal voltage. Overall, a transmission of about 5% has been achieved.  $\text{FeH}^-$  molecules are injected at typical beam currents of 15–20 nA. The isobar  $^{60}\text{Ni}$  is an interference in the detection of  $^{60}\text{Fe}$ . The isobar suppression capability of the detection system was measured with a  $^{58}\text{Fe}/^{58}\text{Ni}$  beam using the multi-anode gas ionisation detector. At 60 MeV, Ni suppression of  $4 \times 10^{-6}$  has been achieved [34]. Thus, and due to the fact that with the use of  $\text{FeH}^-$  beams the interfering isobar  $^{60}\text{Ni}$  is suppressed substantially, a detection limit of  $10^{-12}$  seems possible.

#### 5. Conclusions

The Zurich AMS facility offers a great variety of ion beam techniques to a large community of internal and external users. Various projects in the different fields of AMS applications have benefited from the continuous progress made in measurement techniques and in system operation. Routine AMS work and the challenge of further

improvements in the application of detection techniques have complemented one another.

### Acknowledgements

This work is financially supported by the Swiss National Science Foundation.

### References

- [1] M. Suter, R. Balzer, B. Bonani and W. Wölfli, *IEEE Trans. Nucl. Sci.* NS-28(2) (1981) 1475.
- [2] W. Wölfli, G. Bonani, M. Suter, R. Balzer, M. Nessi, Ch. Stoller, J. Beer, H. Oeschger and M. Andree, *Radiocarbon* 25(2) (1983) 745.
- [3] M. Suter, R. Balzer, B. Bonani, M. Nessi, C. Stoller, W. Wölfli, M. Andree, J. Beer and H. Oeschger, *IEEE Trans. Nucl. Sci.* NS-30(2) (1983) 1528.
- [4] G. Bonani, H.J. Hofmann, E. Morenzoni, M. Nessi, M. Suter and W. Wölfli, *Radiocarbon* 28(2A) (1986) 246.
- [5] M. Suter, J. Beer, D. Billeter, G. Bonani, H.J. Hofmann, H.-A. Synal and W. Wölfli, *Nucl. Instr. and Meth. B* 40/41 (1989) 734.
- [6] M. Suter, G. Bonani, Ch. Stoller and W. Wölfli, *Nucl. Instr. and Meth. B* 5 (1984) 251.
- [7] G. Bonani, P. Ebehardt, H.J. Hofmann, Th. Niklaus, M. Suter, H.-A. Synal and W. Wölfli, *Nucl. Instr. and Meth. B* 52 (1990) 338.
- [8] Th. Niklaus, G. Bonani, Z. Guo, M. Suter and H.-A. Synal, *Nucl. Instr. and Meth. B* 92 (1994) 115.
- [9] M. Suter, R. Balzer, G. Bonani and W. Wölfli, *Nucl. Instr. and Meth. B* 5 (1984) 242.
- [10] R. Balzer, *Nucl. Instr. and Meth. B* 5 (1984) 247.
- [11] H.-A. Synal, G. Bonani, R.C. Finkel, Th. Niklaus, M. Suter and W. Wölfli, *Nucl. Instr. and Meth. B* 56/57 (1991) 864.
- [12] R. Balzer, G. Bonani, M. Nessi, Ch. Stoller, M. Suter and W. Wölfli, *Nucl. Instr. and Meth. B* 5 (1984) 204.
- [13] Th. Niklaus, W. Baur, G. Bonani, M. Suter, H.-A. Synal and W. Wölfli, *Rev. Sci. Instr.* 63(4) (1991) 2485.
- [14] Th. Niklaus, F. Ames, G. Bonani, M. Suter and H.-A. Synal, *Nucl. Instr. and Meth. B* 92 (1994) 96.
- [15] M. Döbeli, R. Ender, U. Fischer, M. Suter, H.-A. Synal and D. Vetterli, *Nucl. Instr. and Meth. B* 94 (1994) 388.
- [16] R.M. Ender, M. Döbeli, P. Nebiker, M. Suter, H.-A. Synal and D. Vetterli, *Proc. SIMS 10*, eds. Benninghoven et al. (Wiley, New York, 1996).
- [17] M. Döbeli, P.W. Nebiker, M. Suter, H.A. Synal, M. Suter and D. Vetterli, *Nucl. Instr. and Meth. B* 85 (1994) 770.
- [18] R.M. Ender, M. Döbeli, M. Suter and H.-A. Synal, these Proceedings (AMS-7), *Nucl. Instr. and Meth. B* 123 (1997) 575.
- [19] H.-A. Synal, J. Beer, G. Bonani, H.J. Hofmann, M. Suter and W. Wölfli, *Nucl. Instr. and Meth. B* 29 (1987) 146.
- [20] U. Zoppi, P.W. Kubik, M. Suter, H.-A. Synal, H.R. vonGuntten and D. Zimmermann, *Nucl. Instr. and Meth. B* 92 (1994) 142.
- [21] M.J.M. Wagner, H.A. Synal and M. Suter, *Nucl. Instr. and Meth. B* 89 (1994) 266.
- [22] M. Nessi, E. Morenzoni, M. Suter, G. Bonani, H.J. Hofmann, C. Stoller and W. Wölfli, *Nucl. Instr. and Meth. B* 5 (1984) 238.
- [23] G. Bonani, J. Beer, H.J. Hofmann, H.-A. Synal, M. Suter, W. Wölfli, C. Pfeleiderer, B. Kromer, C. Junghans and K.O. Munnich, *Nucl. Instr. and Meth. B* 29 (1987) 87.
- [24] M. Suter, R. Balzer, G. Bonani, H.J. Hofmann, E. Morenzoni, E. Nessi and W. Wölfli, *Nucl. Instr. and Meth. B* 5 (1984) 117.
- [25] H.-A. Synal, J. Beer, G. Bonani, Ch. Lukaszczuk and M. Suter, *Nucl. Instr. and Meth. B* 92 (1994) 79.
- [26] M.J.M. Wagner, B. Dittrich-Hannen, H.-A. Synal, M. Suter and U. Schotterer, *Nucl. Instr. and Meth. B* 113 (1996) 490.
- [27] B. Dittrich-Hannen, F. Ames, M. Suter, M. Wagner, Ch. Schnabel, R. Michel, U. Herpers and E. Günther, *Nucl. Instr. and Meth. B* 113 (1996) 453.
- [28] H. Artigas et al., *Nucl. Instr. and Meth. B* 79 (1993) 617.
- [29] M.J.M. Wagner, H.A. Synal, M. Suter and J.-L. Debrun, *Nucl. Instr. and Meth. B* 99 (1995) 519.
- [30] W.E. Meyerhof, A. Rüetschi, Ch. Stoller, M. Stöckli and W. Wölfli, *Phys. Rev. A* 20 (1979) 154.
- [31] H.J. Hofmann, G. Bonani, M. Suter, W. Wölfli, D. Zimmermann and H.R. von Gunten, *Nucl. Instr. and Meth. B* 52 (1990) 544.
- [32] P. Gartenmann, R. Golser, P. Haas, W. Kutschera, M. Suter, H.-A. Synal, M. Wagner and E. Wild, *Nucl. Instr. and Meth. B* 114 (1996) 125.
- [33] P. Haas, P. Gartenmann, R. Golser, W. Kutschera, M. Suter, H.-A. Synal, M. Wagner, E. Wild and G. Winkler, *Nucl. Instr. and Meth. B* 114 (1996) 131.
- [34] P. Gartenmann, Ch. Schnabel, M. Suter and H.-A. Synal, these Proceedings (AMS-7), *Nucl. Instr. and Meth. B* 123 (1997) 132.